

17. Gusev G M et al., in *Proc. of 12th Intern. Conf. High Magnetic Fields in Semiconductors Physics, Würzburg, 1996* (Eds G Landwehr, W Ossau) (Singapore: World Scientific, 1997) p. 391
18. Lee P A, Ramakrishnan T V *Rev. Mod. Phys.* **57** 287 (1985)
19. Ovadyahu Z, Imry Y *J. Phys. C* **18** L19 (1985)
20. Imry Y, Stern A, Sivan U *Europhys. Lett.* **39** 639 (1997)
21. Efros A L *Solid State Commun.* **65** 1281 (1988)

## Chaotic quantum transport in superlattices

T M Fromhold, A A Krokhin, P B Wilkinson, A E Belyaev, C R Tench, S Bujkiewicz, F W Sheard, L Eaves, M Henini

**Abstract.** We report a new type of quantum chaotic system in which the classical Hamiltonian originates from the intrinsically quantum mechanical nature of the device. The system is a semiconductor superlattice in a magnetic field. The energy–momentum dispersion curves can be used to calculate semiclassical orbits for electrons confined to a single miniband. When a magnetic field is applied along the superlattice axis ( $x$ -direction), the electrons perform Bloch oscillations along the axis with cyclotron motion in the orthogonal plane. But when the magnetic field is tilted away from the  $x$ -direction, the orbits are chaotic, and have a spatial width along the superlattice axis, which is much larger than the amplitude of the Bloch oscillations. This is because the tilted field transfers momentum between the  $x$ - and  $z$ -directions, thereby delocalizing the electron path. This type of chaotic dynamics is *fundamentally different* to that identified in our previous studies of double–barrier resonant tunneling diodes. We investigate the relation between the orbits of the effective Hamiltonian, and the quantum states of the superlattice. In the regime of strong chaos, the wave functions have a highly diffuse structure which extends across many periods of the superlattice, just like the corresponding classical orbits. This chaos-induced delocalization increases the current flow through real devices. By contrast, in the stable domain the electron orbits remain localized along the paths of particular quasi-periodic orbits. We use theoretical and experimental current–voltage curves to show how the onset of chaos manifests itself in the transport properties of two- and three-terminal superlattice structures, and identify current oscillations associated with classical resonances. We also consider analogies with ultra-cold atoms in an optical lattice with a tilted harmonic trap.

We investigate the semiclassical motion of electrons confined to the lowest miniband of a GaAs/(AlGa)As superlattice with a high magnetic field. Tilting the magnetic field away from the superlattice axis induces a transition from stable regular motion to chaotic dynamics which have an intrinsically quantum-mechanical origin associated with the miniband dispersion relation. The onset of chaos delocalizes the semiclassical orbits and corresponding quantized eigenstates. We

use a classical kinetic formalism to calculate the electron drift velocity versus applied bias voltage, and find that chaos-induced orbital delocalization can produce a large increase in the electrical conductivity.

Most experimental studies of the quantum properties of systems with chaotic classical dynamics have been performed either on atoms or on low-dimensional semiconductor structures [1]. The first experiments were performed on highly-excited hydrogenic atoms in a magnetic field, and revealed periodic fluctuations in the photo-absorption spectra, associated with unstable periodic electron paths [2, 3]. These orbits modulate the energy level density, and produce ‘scarred’ wave functions in which the probability density is concentrated along the classical path [4, 5]. More recently, ultra-cold atoms in a phase-modulated optical lattice, formed using two counter-propagating laser beams to set up an electromagnetic standing wave [6], have provided experimental evidence for dynamical localization in a quantum-mechanical ‘kicked rotor’ [7]. In semiconductor physics, chaotic electron transport has been explored in two-dimensional quantum dots [1, 8, 9], antidot arrays [10], and in resonant tunneling diodes (RTDs) [1, 11–19]. The RTDs contain a square potential well, in which electrons follow chaotic classical paths when a tilted magnetic field is applied [1, 11–19]. In the regime of strong chaos, scarred states in the well generate series of resonant peaks in measured tunneling characteristics [12, 15].

In this paper, we consider how semiconductor superlattices (SLs) with a tilted magnetic field can be used to provide a new type of quantum chaotic system that is accessible to experiment. In contrast to previous structures that have been used to study quantum chaos, the effective classical Hamiltonian for electron motion in the SLs has an intrinsically quantum-mechanical origin associated with the electronic energy bands. For low electric fields, SLs have well-defined minibands. The energy–wavevector dispersion relations define an effective Hamiltonian that determines semiclassical [20] orbits for electrons confined to a single miniband. Our calculations for this system show that tilting an applied magnetic field  $\mathbf{B}$  at an angle  $\theta$  to the SL axis induces a transition from stable to chaotic classical motion. The onset of chaos delocalizes both the classical orbits and the corresponding quantum wave functions, and thereby increases the electron drift velocity.

The potential energy of an electron in a SL structure is schematically shown in Fig. 1. Here we consider GaAs/(AlGa)As SLs containing barriers of width  $b = 1.25$  nm and wells of width  $w = 9.5$  nm. The SL period  $a = b + w$ . The Al fraction is taken to be either 0.3, for which the miniband width  $\Delta = 26$  meV, or 1, which gives  $\Delta = 8$  meV. We have investigated electron transport in the first miniband of the SL, using a tight-binding approximation for the energy–wavevector dispersion relation

$$E(\mathbf{k}) = \frac{\Delta(1 - \cos k_x a)}{2} + \frac{\hbar^2(k_y^2 + k_z^2)}{2m^*},$$

where  $m^* = 0.07m_e$  is the electron effective mass for motion in the  $(y, z)$  plane. The  $E(\mathbf{k})$  relation defines an effective Hamiltonian for electron motion in electric and magnetic fields that are small enough to preserve the miniband structure. This Hamiltonian is obtained from  $E(\mathbf{k})$  by adding the electrostatic potential energy due to the electric field  $\mathbf{F} = (-F, 0, 0)$  and making the substitution  $\hbar\mathbf{k} = \mathbf{p} \rightarrow \mathbf{p} + e\mathbf{A} = m^*\mathbf{v}$ , where

T M Fromhold, A A Krokhin, P B Wilkinson, A E Belyaev, C R Tench, S Bujkiewicz, F W Sheard, L Eaves, M Henini School of Physics and Astronomy, University of Nottingham, Nottingham NG7 2RD, UK  
A A Krokhin Universidad Autonoma de Puebla, Puebla, Mexico  
S Bujkiewicz Institute of Physics, Wrocław University of Technology, Wybrzeże, Wyspińskiego 27, 50–370, Poland

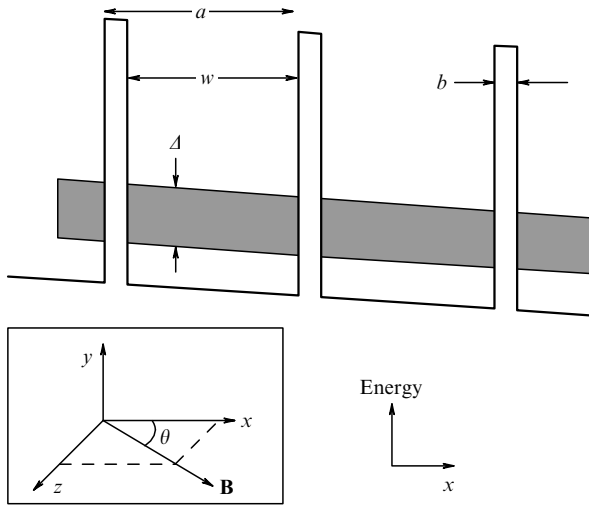


**Figure 1.** Schematic conduction band diagram showing energy versus position  $x$  for an electron in a SL under bias. Shaded region indicates energy range of the lowest electronic miniband. Inset shows orientation of tilted magnetic field relative to the  $x$ -direction, which is parallel to SL axis.

$\mathbf{p}$  is the canonical momentum,  $\mathbf{v} = \hbar^{-1} \partial E / \partial \mathbf{k}$  is the electron velocity, and  $\mathbf{A}$  is the magnetic vector potential. With the magnetic field  $\mathbf{B}$  applied in the  $(x, z)$  plane (Fig. 1, inset), we take

$$\mathbf{A} = (0, xB \sin \theta - zB \cos \theta, 0).$$

The canonical momentum component  $p_y$  is then constant and the problem reduces to two-dimensional motion in the  $(x, z)$  plane with an effective potential energy [21]

$$U(x, z) = \frac{e^2 B^2}{2m^*} [x \sin \theta - (z - z_0) \cos \theta]^2 - eFx, \quad (1)$$

where  $z_0 = p_y / eB \cos \theta$ . The form of the classical orbits is independent of  $z_0$  and the total electron energy, which we both set to zero. We have calculated these orbits by solving Hamilton's equations numerically using a fourth-order Runge-Kutta method [21].

Figure 2 shows electron orbits in a GaAs/(Al<sub>0.3</sub>Ga<sub>0.7</sub>)As SL. Note that Figs 2a–c show the trajectories in real  $(x, z)$  space, whilst Figs 2d–f show the orbits in  $(k_x, k_z)$  space. For  $\theta = 0^\circ$  the Hamiltonian is separable. The electrons execute cyclotron motion about the  $z$ -axis and Bloch oscillations, of angular frequency  $\omega_B$ , along the  $x$ -direction (Fig. 2a). For  $\theta \neq 0^\circ$ , the orbital motion changes from regular to chaotic as  $B$  is increased from 0 T. When  $\theta = 40^\circ$  and  $B = 0.6$  T (Fig. 2b), most orbits are stable and qualitatively similar to that in Fig. 2a. But when  $B$  is increased to 1.5 T, the orbits become chaotic (Fig. 2c). Because the tilted magnetic field transfers momentum between the  $x$ - and  $z$ -directions, these orbits extend much further along the SL axis than the Bloch oscillations at  $\theta = 0^\circ$ , whose amplitude is limited by the conservation of energy for motion along the  $x$ -direction. The electron orbits in  $\mathbf{k}$ -space show the transition to chaos in a different way. In an extended miniband scheme, the Bloch oscillations at  $\theta = 0^\circ$  produce a sinusoidal  $k_z$  versus  $k_x$  plot (Fig. 2d). The stable orbits found for  $\theta = 40^\circ$  and  $B = 0.6$  T generate quasi-periodic oscillations in  $\mathbf{k}$ -space

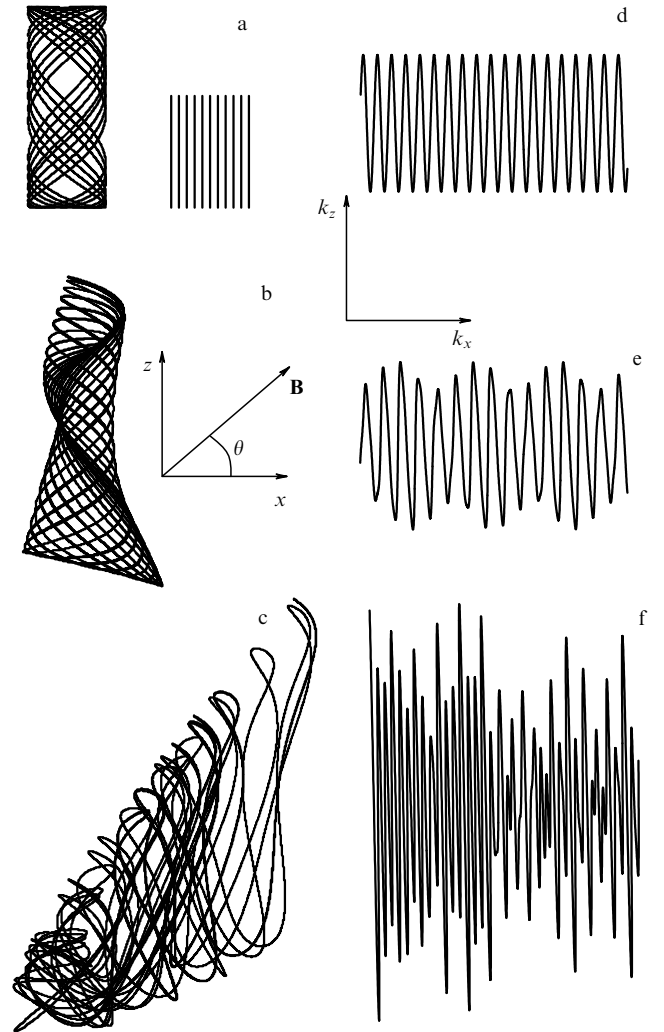


**Figure 2.** Classical electron orbits in  $(x, z)$  plane (a–c) and  $(k_x, k_z)$  plane (d–f) (axes are shown in the insets) with  $F = 2.4 \times 10^5$  Vm<sup>-1</sup>;  $B = 0.6$  T,  $\theta = 0^\circ$  (a, d);  $B = 0.6$  T,  $\theta = 40^\circ$  (b, e);  $B = 1.5$  T,  $\theta = 40^\circ$  (c, f). Vertical lines show positions of barriers in SL layer and indicate scale.

(Fig. 2e). The amplitude of these oscillations is modulated by beating between the cyclotron and Bloch frequencies. As the magnetic field is increased to 1.5 T, the  $\mathbf{k}$ -space trajectories break into chaotic oscillations (Fig. 2f).

We emphasize that the chaotic dynamics have a fundamentally different origin to those of electrons in RTDs with a tilted magnetic field. In the RTDs, chaos is generated by collisions with the well walls which interrupt the electron motion at irregular times [11–19]. By contrast, electrons in a SL with tilted  $\mathbf{B}$  exhibit chaotic dynamics because they have an anisotropic and energy-dependent effective mass due to the different dispersion relations for motion parallel and perpendicular to the SL axis. Tilting  $\mathbf{B}$  couples the motion along the  $x$ - and  $z$ -directions and thereby induces chaotic dynamics. The classical orbits considered here are also unrelated to the chaotic oscillations of charge domains in driven SL structures [22, 23].

The transition to chaos in this system is characterized by a rich mixed stable-chaotic classical phase space. This can be seen from Fig. 3 which shows a Poincaré section (a slice through the classical phase space) calculated for electrons in a GaAs/(Al<sub>0.3</sub>Ga<sub>0.7</sub>)As SL. To construct the section, electrons

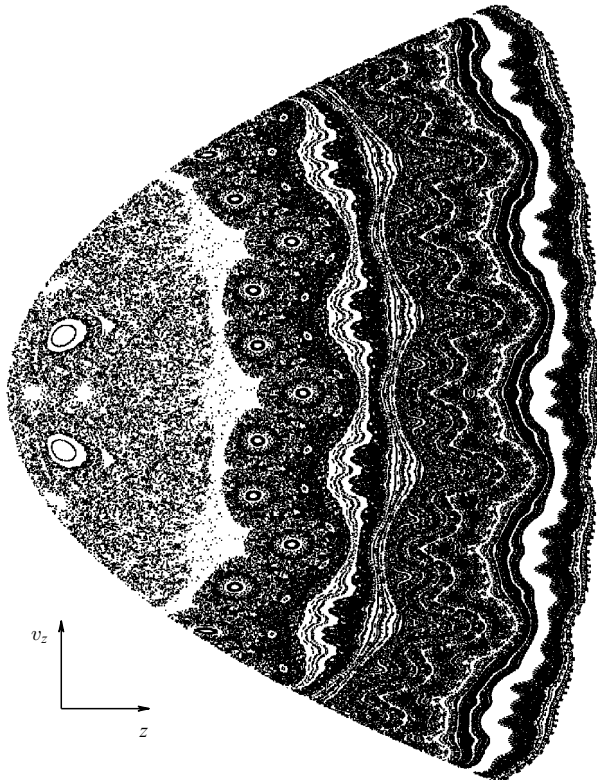


**Figure 3.** Poincaré section showing  $(z, v_z)$  values (arbitrary units) when  $v_x = 0$ , calculated for  $B = 2.3$  T,  $\theta = 60^\circ$ , and  $F = 2.4 \times 10^5$  Vm $^{-1}$ .

are launched with a range of starting velocities at  $\theta = 60^\circ$  and  $B = 2.3$  T. The scattered points show coordinate  $z$  and velocity  $v_z$  at each turning point along the  $x$ -direction (whenever  $v_x = 0$ ). The phase space contains a complex hierarchy of stable islands that disintegrate to form a chaotic sea as  $B$  is increased. Stable islands embedded within a chaotic sea can be seen most clearly towards the left-hand side of the plot.

An extensive body of theoretical work has shown that the unstable but periodic orbits of a chaotic classical system give rise to periodic fluctuations in the energy level density [1] and scar subsets of wave functions [1, 4, 15]. But it is unclear how the quantized states of a SL in a tilted magnetic field will relate to chaotic electron orbits which themselves originate from the intrinsically quantum-mechanical nature of minibands. As a first step in exploring this question, we have calculated quantized states for a GaAs/(Al $_{0.3}$ Ga $_{0.7}$ )As SL using a technique similar to that developed for RTDs in Refs [12, 15]. The SL system is ideal for theoretical analysis because for our chosen gauge the dynamics, classical or quantum, become two-dimensional. The eigenfunctions can then be expanded in a basis of Wannier functions along the SL axis with simple harmonic oscillator (Landau) states along the  $z$ -direction [21]. For the low energies and fields considered here, interminiband coupling is negligible and so we only include Wannier states for the first miniband in our basis. Figure 4a shows the regular antinode pattern of a Wannier–Stark eigenfunction at  $\theta = 0^\circ$ . The probability density is concentrated within the corresponding classical orbit (Fig. 2a), and has a width of  $\sim \Delta/eF = 5a$  along the  $x$ -direction. Figure 4b shows the probability distribution of an eigenfunction calculated in a regime of chaotic classical dynamics at  $\theta = 40^\circ$ . Just like the chaotic classical paths, the wave

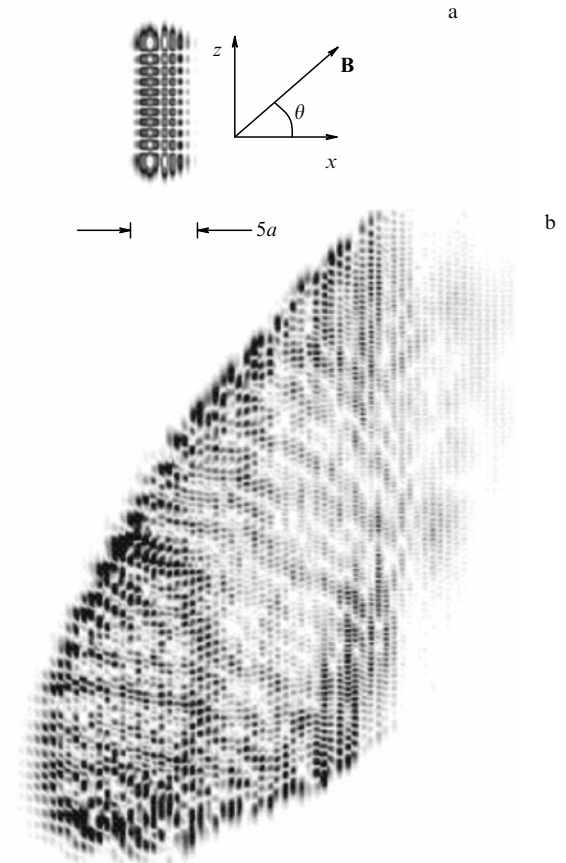


**Figure 4.** Probability density plots (white = 0) of electron eigenstates for  $F = 4.9 \times 10^5$  Vm $^{-1}$  and (a)  $B = 0.6$  T,  $\theta = 0^\circ$  showing amplitude  $5a$  of corresponding Bloch oscillation, (b)  $B = 1.5$  T,  $\theta = 40^\circ$ .

function has a highly irregular and diffuse structure which extends across many ( $\sim 50$ ) SL periods. Since the onset of chaos delocalizes both the classical orbits and the corresponding quantized states, we expect that it will give rise to an experimentally-observable increase in the electrical conductivity of the SL.

To quantify this effect, we have calculated the electron drift velocity  $v_d$  along the  $x$  direction as a function of the bias voltage  $V$  ( $F = 5 \times 10^6$  V Vm $^{-1}$  with  $V$  in volts) dropped across a 40-period GaAs/AlAs SL. Our calculations used the classical kinetic formula

$$v_d(V) \propto \frac{1}{\tau} \sum_s \int_0^\infty \exp\left(\frac{-t}{\tau}\right) v_x^s(t) dt, \quad (2)$$

where the summation is over all trajectories  $s$  consistent with the electron injection energy,  $v_x^s(t)$  describes the time evolution of the  $x$  component of velocity (determined by numerical solution of the classical Hamiltonian [21]) for an electron in the  $s$ th trajectory, and the electron scattering time  $\tau = 1$  ps is obtained from experiment [24].

Figure 5 shows  $v_d(V)$  curves calculated for electrons starting from rest at the bottom of the lowest (8 meV wide) miniband. We emphasize that similar results are obtained for a wide range of injection energies. When  $\theta = 0^\circ$ , the electrons perform Bloch oscillations along the SL axis (Fig. 2a). The  $v_d(V)$  plot (solid curve in Fig. 5) peaks at the voltage  $V_B \approx 12$  mV for which  $\omega_B = 1/\tau$  [25]. The dashed (dotted) traces in Fig. 5 show  $v_d(V)$  curves calculated for  $\theta = 45^\circ$  and

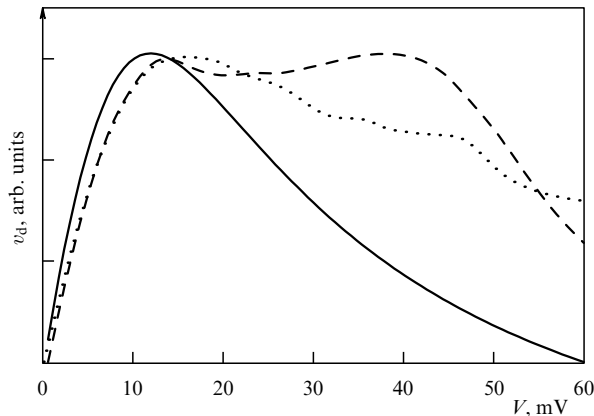


**Figure 5.**  $v_d(V)$  curves calculated for  $B = 5$  T,  $\theta = 0^\circ$  (solid curve),  $B = 1.5$  T,  $\theta = 45^\circ$  (dashed curve) and  $B = 5$  T,  $\theta = 45^\circ$  (dotted curve).

$B = 1.5$  T (5 T). For  $V \lesssim V_B$ , the shape of both of these curves is similar to that for  $\theta = 0^\circ$ . Moreover, in this low voltage regime, tilting the magnetic field has little effect on the magnitude of  $v_d$ . This is because when  $V$  is small, the electrons travel such a short distance before scattering that it is hard to distinguish between the regular ( $\theta = 0^\circ$ ) and chaotic ( $\theta \neq 0^\circ$ ) trajectories, and so both types of orbit have similar drift velocities. In a tilted magnetic field,  $v_d$  is slightly lower because the field component parallel to the potential barriers deflects the electron trajectories, thus reducing the average velocity along the SL axis [26]. At high voltages, by contrast, the mean free path of the electrons is long enough for the differences between regular and chaotic orbits to influence the transport properties of the SL. Electrons in spatially extended chaotic trajectories (Fig. 2c) travel further along the SL before scattering, and therefore have higher drift velocities. This should raise the electrical conductivity measured in electron transport experiments.

In a tilted magnetic field, the  $v_d(V)$  curves contain weak oscillatory structure which can be seen most easily in the dotted (5 T,  $45^\circ$ ) trace in Fig. 5. The origin of these oscillations seems to involve resonances between the classical cyclotron and Bloch frequencies when  $\theta = 0^\circ$ , and will be analyzed in detail elsewhere [27].

This work was funded by EPSRC UK and the Royal Society of London. T M F was supported by an EPSRC Advanced Fellowship. S B, A A K are grateful to the British Council (Royal Society) for financial support.

## References

1. For a review see Stockmann H-J *Quantum Chaos – An Introduction* (Cambridge: Cambridge Univ. Press, 1999)
2. Garton W R S, Tomkins F S *Astrophys. J.* **158** 839 (1969)
3. Holle A et al. *Phys. Rev. Lett.* **61** 161 (1988)
4. Heller E J *Phys. Rev. Lett.* **53** 1515 (1984)
5. Wintgen D, Hönl A *Phys. Rev. Lett.* **63** 1467 (1989)
6. For a review see Meacher D R *Contemp. Phys.* **39** 329 (1998)
7. Moore F L et al. *Phys. Rev. Lett.* **73** 2974 (1994)
8. Marcus C M et al. *Phys. Rev. Lett.* **69** 506 (1992)
9. Chang A M et al. *Phys. Rev. Lett.* **73** 2111 (1994)
10. Weiss D et al. *Phys. Rev. Lett.* **70** 4118 (1993)
11. Fromhold T M et al. *Phys. Rev. Lett.* **72** 2608 (1994)
12. Fromhold T M et al. *Phys. Rev. Lett.* **75** 1142 (1995)
13. Shepelyansky D L, Stone A D *Phys. Rev. Lett.* **74** 2098 (1995)
14. Müller G et al. *Phys. Rev. Lett.* **75** 2875 (1995)
15. Wilkinson P B et al. *Nature* **380** 608 (1996)
16. Narimanov E E, Stone A D, Boebinger G S *Phys. Rev. Lett.* **80** 4024 (1998)
17. Narimanov E E, Stone A D *Phys. Rev. Lett.* **80** 49 (1998)
18. Saraga D S, Monteiro T S *Phys. Rev. Lett.* **81** 5796 (1998)
19. Bogomolny E B, Rouben D C *Europhys. Lett.* **43** 111 (1998)
20. Here we refer to electron transport through the minibands as ‘semiclassical’ because the effective classical equations of motion are derived by considering the response of a quantum-mechanical wavepacket to force fields which are spatially slowly varying. Henceforth we label the orbits obtained from these equations as classical
21. Bujkiewicz S et al. *Physica E* **6** 306 (2000)
22. Bulashenko O M, Bonilla L L *Phys. Rev. B* **52** 7849 (1995)
23. Zhang Y H et al. *Phys. Rev. Lett.* **77** 3001 (1996)
24. Rauch C et al. *Phys. Rev. Lett.* **81** 3495 (1998)
25. Esaki L, Tsu R *IBM J. Res. Dev.* **14** 61 (1970)
26. Hutchinson H J et al. *J. Appl. Phys.* **75** 320 (1994)
27. Fromhold T M et al. (to be published)

## Quasiclassical memory effects: anomalous transport properties of two-dimensional electrons and composite fermions subject to a long-range disorder

F Evers, A D Mirlin, D G Polyakov, P Wölfle

**Abstract.** We have studied the ac response and magnetoresistance of a two-dimensional electron gas in high-mobility samples in the presence of smooth disorder, with emphasis on the composite-fermion description of a half-filled Landau level. We have found that the low- $\omega$  behavior of the ac conductivity  $\sigma(\omega)$  is governed by memory effects associated with return processes that are neglected in Boltzmann transport theory: the return-induced correction to  $\text{Re } \sigma$  exhibits a kink  $\propto |\omega|$ . It is shown that the non-Markovian quasiclassical kinetics leads to a strong magnetoresistance  $\Delta\rho_{xx}$ . We argue that the quasiclassical memory effects account for the positive  $\Delta\rho_{xx}$  observed at small deviations from half-filling. At a larger deviation, the positive magnetoresistance is followed by a sharp falloff of  $\rho_{xx}$ .

Recently, there has been a revival of interest in *quasiclassical* transport properties of a two-dimensional electron gas (2DEG). This is motivated by the realization that the classical dynamics in a disordered system constitutes in fact far more than the idealized Drude picture and, to describe the transport properties of the system, one has sometimes to completely abandon theories based on the Boltzmann equation. In Boltzmann transport theory, formulated in terms of a collision integral, quasiclassics leads to the Drude results: analytical behavior of the ac conductivity  $\sigma(\omega)$  at  $\omega \rightarrow 0$ , zero magnetoresistance (MR), etc. It has been demonstrated, however, that quasiclassical *memory effects*, neglected in the conventional Boltzmann approach, yield a

F Evers, A D Mirlin, P Wölfle Institut für Theorie der Kondensierten Materie, Universität Karlsruhe, 76128 Karlsruhe, Germany  
A D Mirlin, D G Polyakov, P Wölfle Institut für Nanotechnologie, Forschungszentrum Karlsruhe, 76021 Karlsruhe, Germany;  
A D Mirlin Petersburg Nuclear Physics Institute, 188350 St. Petersburg, Russian Federation  
D G Polyakov A F Ioffe Physical-Technical Institute, 194021 St. Petersburg, Russian Federation